Quantum Yields and Reaction Times of Photochromic Diarylethenes: Non-Adiabatic Ab Initio Molecular Dynamics for Normal- and Inverse-Type.

ARTICLE *in* THE JOURNAL OF PHYSICAL CHEMISTRY A · AUGUST 2014

Impact Factor: 2.69 · DOI: 10.1021/jp506316w · Source: PubMed

2 AUTHORS:

Christian Wiebeler
Universität Paderborn
14 PUBLICATIONS **47** CITATIONS
SEE PROFILE

Stefan Schumacher
Universität Paderborn
75 PUBLICATIONS **497** CITATIONS
SEE PROFILE

THE JOURNAL OF PHYSICAL CHEMISTRY A

Article

pubs.acs.org/JPCA

Quantum Yields and Reaction Times of Photochromic Diarylethenes: Nonadiabatic Ab Initio Molecular Dynamics for Normal- and Inverse-Type

Christian Wiebeler[†] and Stefan Schumacher*[,†]

[†]Physics Department and Center for Optoelectronics and Photonics Paderborn (CeOPP), Universität Paderborn, Warburger Strasse 100, 33098 Paderborn, Germany

Supporting Information

ABSTRACT: Photochromism is a light-induced molecular process that is likely to find its way into future optoelectronic devices. In further optimization of photochromic materials, light-induced conversion efficiencies as well as reaction times can usually only be determined once a new molecule was synthesized. Here we use nonadiabatic ab initio molecular dynamics to study the electrocyclic reaction of diarylethenes, comparing normal- and inverse-type systems. Our study highlights that reaction quantum yields can be successfully predicted in accord with experimental findings. In particular, we find that inverse-type diarylethenes show a significantly higher reaction quantum yield and cycloreversion on times typically as short as 100 fs.

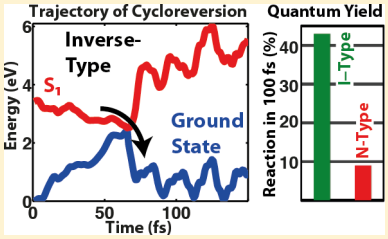

I. INTRODUCTION

In photochromic molecular materials, illumination with light leads to a reversible transformation of a single chemical species between two forms with different optical properties. The transformation is induced all-optically, in one or two directions.[1] This type of light-induced functionality is typically not found in materials used in photonic systems. Integration of photochromic molecules therefore poses a promising route to the design of novel optoelectronic and photonic devices.[2,3] Photochromic spiropyrans were for example used to functionalize single-walled carbon nanotubes,[4] and azobenzene-based polyelectrolytes were incorporated into tunable semiconductor microresonator structures.[5] Among the different photochromic materials that can reversibly and optically be switched between both of their forms, diarylethenes excel with high fatigue resistance, thermal stability, and high quantum yields.[6,7] Showing their photochromic functionality even in solid films, diarylethenes are promising to be used in solid-state photonic hybrid structures.[8,9] Potential applications include optical memories[10] and multifunctional all-optical switches.[7,11,12]

For diarylethenes it was noted that they can be further divided into two subcategories: (i) normal-type diarylethenes in which the ethylene bridge is connected on both sides to a carbon atom of the thiophene ring that is in the 3-position; (ii) inverse-type diarylethenes in which the ethylene bridge is connected to a carbon atom in the 2-position. The two structures are depicted in Scheme 1. Normal-type (N-type) and inverse-type (I-type) diarylethenes have many of their favorable properties in common, e.g., the same reactive center. However, there are also three main differences. The closed form of N-type diarylethene absorbs light at lower energies than the I-type, which is attributed to the larger conjugation of π-electrons in the former case.[7] For the open forms the situation is reversed.[13] And third and most importantly for prospective applications, the quantum yield of the cycloreversion of I-type was recently found to be significantly higher than for the N-type.[14,15]

Scheme 1. Illustration of the Two Diarylethenes under Study, Normal-Type (Top) and Inverse-Type (Bottom)[a]

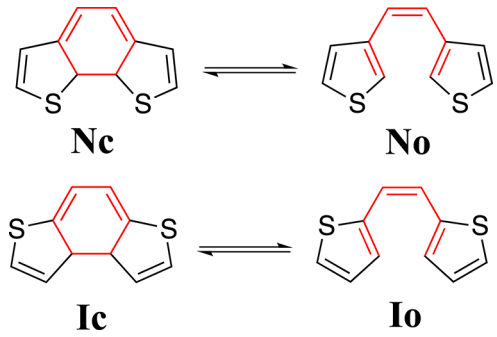

[a]Shown are closed (left) and open (right) ring forms as denoted by the labels. The reactive centers are highlighted, and the photoinduced conversion between open- and closed-ring forms is indicated.

Following photoexcitation of a diarylethene molecule from its thermally stable closed-ring form, the system can undergo an electrocyclic reaction, leading to opening of the central reactive ring (cf. Scheme 1). The electrocyclic photoisomerization of diarylethenes is analogous to the photoisomerization from 1,3-cyclohexadiene (CHD) to 1,3,5-hexatriene (HT). This is shown in Scheme 1. Only the center of the molecule, the CHD/HT-system that is colored in red, is actively involved in the reaction. We note that this center is a well-known textbook

Received: June 25, 2014
Revised: August 19, 2014
Published: August 20, 2014

example for electrocyclic reactions.[16,17] Therefore, the reaction leading to the isomerization is a photochemical 6 electron reaction happening in a conrotatory fashion, as dictated by the Woodward−Hoffmann rules.[18] Upon absorption of visible light, the molecule is in the first excited singlet state. Relaxation leads to a conical intersection between this state and the ground state, leading to an ultrafast reaction and radiationless decay to one of the two stable ground-state structures. For this photochemical isomerization the conical intersection plays a fundamental role.[19]

So far, theoretical studies of the reaction mechanisms of diarylethenes were based on calculated potential energy surfaces with emphasis on N-type forms.[15,20,21] Dynamical studies were limited to the molecular mechanics valence bond method.[22] Generally, only very little work is available on I-type diarylethenes with a notably increasing interest in the past year, both experimentally[23−25] and theoretically.[13,14] Ab initio nonadiabatic dynamics on related systems, e.g., azobenzene[26−28] and stilbene,[29] were calculated. Studies of ab initio nonadiabatic dynamics for diarylethenes were only reported for one specific diarylethene compound.[30] The focus of the present study is on the comparison of qualitative differences in the dynamics of prototypical inverse- and normal-type diarylethenes.

To optimize photochromic materials further, it is crucial to understand the achievable reaction quantum yields and reaction time scales. However, these quantities typically only become accessible after a given substance has been synthesized. From a theoretical point of view, predicting reaction quantum yields involving excited electronic states usually poses a formidable task. Experimentally, reaction time scales are only accessible with advanced spectroscopic techniques. However, these will play an increasingly important role in miniaturized applications in which photochromic functionality is implemented with a few molecules only.[31,32] In this case, the actual molecular reaction times are not overshadowed by the slow overall response of a large molecular ensemble.

In this article, we theoretically investigate the reaction mechanisms in I- and N-type diarylethenes. Our ab initio calculations of the cycloreversion reaction dynamics are based on nonadiabatic trajectory surface hopping (TSH). We demonstrate that this approach gives us direct access to both reaction quantum yields and reaction time scales.

II. METHODS

A. Ground-State Optimization and Vertical Excitation Energies. Optimization of the ground-state structures of the two isomers was carried out using density-functional theory (DFT)[33] with the def2-SVP basis set[34] and the PBE0[35,36] functional. Vibrational frequency analysis confirmed that the structures found are stable minima. Employing the same basis set and the same functional, the excitation energies were calculated with time-dependent DFT (TDDFT)[37] and within the Tamm−Dancoff approximation.[38] To test for convergence regarding the basis set, the same calculaions were repeated using aug-cc-pVTZ[39,40] as the basis set. Furthermore, the excitation energies were also calculated using wave function-based methods allowing benchmarking of the DFT-based results. For this purpose, the open- and closed-ring structures were optimized with RI-CC2[41−45] using the implementation in Turbomole[46] and employing the aug-cc-pVDZ basis set with the corresponding auxiliary basis set[47] and default frozen orbitals. The same basis sets and frozen orbitals were then used to calculate the vertical excitation energies with RI-CC2 and RI-ADC(2).[48−50] Convergence regarding the basis set was again tested by doing the same calculations with the aug-cc-pVTZ basis set. All these calculations were done with Turbomole 6.5.[46]

B. Nonadiabatic Dynamics of the Cycloreversion Reaction. The nonadiabatic ab initio molecular dynamics was calculated following the protocol described in ref 51. As in the static calculations, def2-SVP and PBE0 were used as basis set and functional, respectively. Sampling of the ground state for the rigid closed ring isomers was done using Born−Oppenheimer molecular dynamics. This allows the generation of a swarm of trajectories for the dynamical calculations with different initial conditions. The ground-state trajectories were calculated for a total of 5000 steps with a time step size of 50 au, such that the simulation time was about ∼4.84 ps. A Nosé−Hoover thermostat with a temperature of 300 K and a response time of 500 au was used to simulate the dynamics in the ground state at room temperature. To calculate the nonadiabatic ab initio molecular dynamics starting in the first excited singlet state based on trajectory surface hopping,[52] 100 structures with corresponding nuclear velocities were randomly chosen. A time step of 40 au and a total of 1000 time steps (∼0.97 ps) were used and the TD-DFT in Tamm−Dancoff approximation was employed. The initial conditions sampled from a canonical ensemble were then evolved in the microcanonical ensemble for the nonadiabatic dynamics. No thermostat was used for the nonadiabatic dynamics and furthermore no decoherence is included in these gas phase calculations. The latter might be of importance for systems with slower reaction times or in the case of coupling with a bath.[53] Further details of the implementation of the nonadiabatic dynamics calculations can be found in refs 51 and 54. It is based on linear response time-dependent density-functional theory.[55] TDA alleviates methodological problems[56] of TD-DFT in the vicinity of the conical intersections between ground and first excited state.[57,58] All the nonadiabatic dynamics calculations were done with the parallelization described in ref 59 using the SMP-version of Turbomole 6.5.

The visualization of molecular structures was realized using GaussView.[60]

C. Potential Energy Surfaces. Potential energy surfaces were calculated using the def2-SVP basis set and the PBE0 functional. The scan coordinate was the distance between the two reactive carbon atoms. The structures of the relaxed ground-state scan were used to calculate the vertical excitation energies with TDA. A second relaxed scan was done optimizing the energy of the first excited state employing TDA. To assess the accuracy of the calculated potential energy surfaces, the same kind of calculations was done using a wave function-based method, i.e., RI-CC2 for ground-state optimization with subsequent calculation of vertical excitation energies and optimization of the first excited state. For all wave function-based calculations aug-cc-pVDZ was used as basis set.

III. RESULTS AND DISCUSSION

A. Ground-State Optimization and Vertical Excitation Energies. As a starting point, the stable open- and closed-ring isomers of both types of molecules are optimized and the vertical excitation energies are calculated. This allows the assessment of the accuracy of the basis set and method used in the dynamics and potential energy surface calculations. Results are summarized in Table 1. The results for all TDDFT

dx.doi.org/10.1021/jp506316w | J. Phys. Chem. A 2014, 118, 7816−7823

Table 1. Computed Excitation Energies for Normal- (N) and Inverse-Type (I) Diarylethenes in Their Respective Closed- and Open-Ring Forms As Indicated by the Corresponding Labels Introduced in Scheme 1[a]

	PBE0/SVP (TDA)	PBE0/ aug-cc-pVTZ (TDA)	PBE0/ SVP	PBE0/ aug-cc-pVTZ	ADC(2)/ aug-cc-pVDZ	ADC(2)/ aug-cc-pVTZ	CC2/ aug-cc-pVDZ	CC2/ aug-cc-pVTZ	experiment (N-type: 1 from 61 I-type: 2 from 23)
					N_C				
S_1	3.07	3.00	2.83	2.79	2.85	2.86	2.89	2.90	2.46
S_2	3.81	3.77	3.77	3.74	3.78	3.82	3.76	3.80	
					N_O				
S_1	4.15	4.04	3.97	3.88	4.27	4.34	4.34	4.36	4.09
S_2	4.83	4.77	4.81	4.75	4.95	5.02	4.94	5.02	
					I_C				
S_1	3.47	3.37	3.32	3.23	3.42	3.40	3.43	3.42	2.87
S_2	4.38	4.13	4.35	4.11	4.30	4.35	4.27	4.31	
					I_O				
S_1	3.86	3.77	3.63	3.57	3.82	3.83	3.83	3.85	3.89
S_2	4.70	4.62	4.68	4.61	4.86	4.93	4.86	4.93	

[a]All energies are given in eV. Note that the structures for the diarylethene molecules used in the experiment are different from the structures of the two model diarylethenes; see Supporting Information for the corresponding structures.

calculations are found to be very similar. The smaller basis set, i.e., def2-SVP, leads to small deviations compared to calculations with larger basis sets. However, the error is, apart from one case, not larger than 0.11 eV. Furthermore, the excitation energies obtained with TDA are in general in better agreement with the RI-CC2 calculations than the TDDFT excitation energies. However, the differences between TDDFT and TDA are rather small compared to the accuracy of the DFT-based methods of about 0.2 eV. We note that the latter might be reversed depending on the chosen functional, e.g., using CAM-B3LYP instead of PBE0. We further note that the excitation energies with RI-ADC(2) are in good agreement with RI-CC2, making the more economic RI-ADC(2) method a good candidate for future calculations of low lying excitation energies of larger diarylethenes. In addition, we find it to be sufficient to use the aug-cc-pVDZ basis set for the wave function-based methods. Qualitative trends are correctly reproduced by all the methods used; i.e., the closed-ring form absorbs at lower energy than the open-ring form, the closed-ring form of I-type absorbs at higher energy than the corresponding form of N-type and the open-ring form of I-type absorbs at lower energy than the open-ring form of N-type.

B. Nonadiabatic Dynamics of the Cycloreversion Reaction. In the following, we will investigate the details of the cycloreversion reaction based on ab initio calculations of the nonadiabatic system dynamics (technical details are given in the Methods). In a first step, we sample the molecules' ground states in the closed-ring form and generate 100 initial conditions in the first excited S_1 state of each molecule. Then we compute the systems' time evolution for a swarm of 100 trajectories. In a second step, we extract the quantum yield of the cycloreversion reaction from a statistical evaluation of the computed trajectories.

The main result is shown in Figure 1 for both normal- and inverse-type diarylethenes. It is clearly visible that the quantum yield for I-type diarylethenes with 77% is significantly higher than for N-type diarylethenes with only 55%. To obtain deeper insight into the dynamics of the reaction, one can divide the trajectories in two classes. The first class consists of trajectories that reacted within the first 100 fs, and the second class consists of the remaining trajectories showing slower reactions. For the I-type diarylethene 50% of trajectories belong to the first class,

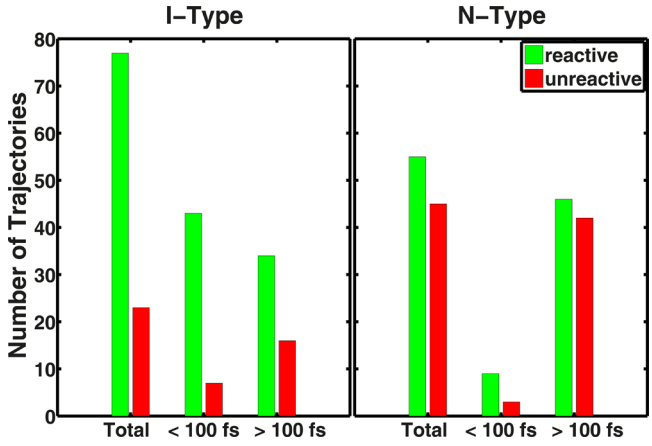

Figure 1. Quantum yield of photoinduced cycloreversion of normal- (N) and inverse-type (I) diarylethenes. The statistics is based on a total of 100 computed trajectories for each type. Given is the total number of trajectories that successfully lead to cycloreversion after relaxation into the S_0 ground state. Out of these trajectories, for I-type a large number already shows a reaction on a very short time scale of only 100 fs. For N-type, the reaction is considerably slower, along with a significantly reduced cycloreversion quantum yield.

whereas only 12% of trajectories reacted within 100 fs for the N-type diarylethene.

In addition to the quantum yields, also the excited-state lifetimes can be obtained using single exponential fits. Using the calculated data, it is possible to determine not only the lifetime for all trajectories but also the lifetimes for reactive and unreactive trajectories as well. The corresponding lifetimes for the CHD/HT-system were reported previously[51] and following the approach described there, we obtain the lifetimes for N- and I-type diarylethenes as listed in Table 2. According to these data the quantum yield for the CHD/HT-system is larger than for the N-type model diarylethene and smaller than for the I-type model diarylethene. The lifetimes for both model diarylethenes are larger, which may be attributed to the thiophene rings that are attached to the CHD backbone. Therefore, it is to be expected that the excited-state lifetime of the larger diarylethene used in experiment[62] is even higher than for the model systems studied here.

dx.doi.org/10.1021/jp506316w | J. Phys. Chem. A 2014, 118, 7816−7823

Table 2. Quantum Yields (%) and Excited-State Lifetimes (ps) for the CHD/HT System, for a Diarylethene Studied in the Experiment and for N- and I-Type Diarylethenes[a]

	QY	τ_{total}	$\tau_{reactive}$	$\tau_{unreactive}$
CHD/HT (Theory[51])	62	0.058	0.043	0.082
N-Type	55	0.28	0.21	0.36
I-Type	77	0.18	0.15	0.30
DAE (Exp.[62])	7.5	1.3		

[a]The lifetimes are obtained by single exponential fits up to the time when 90% of the trajectories have decayed to the ground state. In addition to the lifetime averaged over all trajectories, values are also reported separately for reactive and unreactive trajectories.

A more detailed picture of the reaction can be obtained by looking at the computed trajectories individually. In Figures 2 and 3 we show representative examples of successful cycloreversion reactions for I- and N-type diarylethenes, respectively. Shown are the initial and final molecular geometries together with the time evolution of the energies of the lowest molecular states. Initially, the molecules are in the first excited electronic state and in the ground state after successful cycloreversion, as indicated in the figures. For inverse-type diarylethenes we find that 50% of trajectories reach the ground state within 100 fs. A reaction dynamics this fast we can attribute to the specific topology of the potential energy landscape in the first excited state, which drives the molecule efficiently to the conical intersection (further discussion of the potential energy surfaces is given below). This is also evidenced in Figure 2 in the rapid lowering in energy of the first excited state during the time evolution at early times. For this kind of trajectory we find that the quantum yield for the desired cycloreversion is as high as 86%. In contrast, for trajectories reaching the ground state at times larger than 100 fs, the quantum yield is found to be only 68%. In these cases that show a slower reaction dynamics, the molecule is not driven as efficiently toward the conical intersection between first excited state and ground state as for the fast reaction. All trajectories were found to be in the ground state after 500 fs. Only 23% did not show the desired cycloreversion reaction such that the final geometry was the closed-ring form again. For N-type diarylethenes we only find 12 trajectories that show a reaction within the first 100 fs. The cycloreversion quantum yield for this kind of trajectory is rather high with about 75%. The remaining 88 trajectories reached the ground state at times later than 100 fs, with a reduced quantum yield of about 52%. Four trajectories did not reach the ground state within the total time of the simulation. Inspecting the trajectory in Figure 3, we do not find a pronounced reduction of the energy of the first excited state during the time evolution. In contrast, after a first relaxation in the first excited state, for the N-type diarylethene an energetic barrier has to be overcome to reach the conical intersection leading to the ground state. Therefore, the normal-type molecule is not driven efficiently toward the conical intersection, explaining the lower quantum yield and higher reaction time compared to I-type molecules. This different behavior might be attributed to the different topography of the conical intersections involved[63,64] that have an impact on the effectiveness of photochemical reactions[65] and excited-state lifetimes.[66]

In Figures 4 and 5, we show additional examples of computed trajectories. Figure 4 shows an example of one of the 50 trajectories for I-type diarylethenes that do not react within the first 100 fs. In this case, the I-type molecule is not driven as efficiently toward the conical intersection as is the case for the trajectory shown in Figure 2. Figure 5 shows one of the 12 trajectories for N-type diarylethene that reacts within the first 100 fs. Even in this case, a small energy barrier has to be overcome to reach the conical intersection, which is the same as for the trajectory shown in Figure 3. Both trajectories pass through the conical intersection and relax back to the initial closed-ring ground-state structure.

Videos showing the computed time-evolution of the molecular geometries for these four different types of trajectories are available online as Supporting Information.

On a more technical note, we find that as long as the molecule is in the first excited state, this state is significantly lower in energy than the second excited state. After the jump into the electronic ground state, however, both of the excited-state energies come very close and sometimes are even almost degenerate. We believe that this does not significantly influence the computed dynamics as it only occurs when the system is in the ground state, which is always very well separated from the excited states. We would further like to note that the

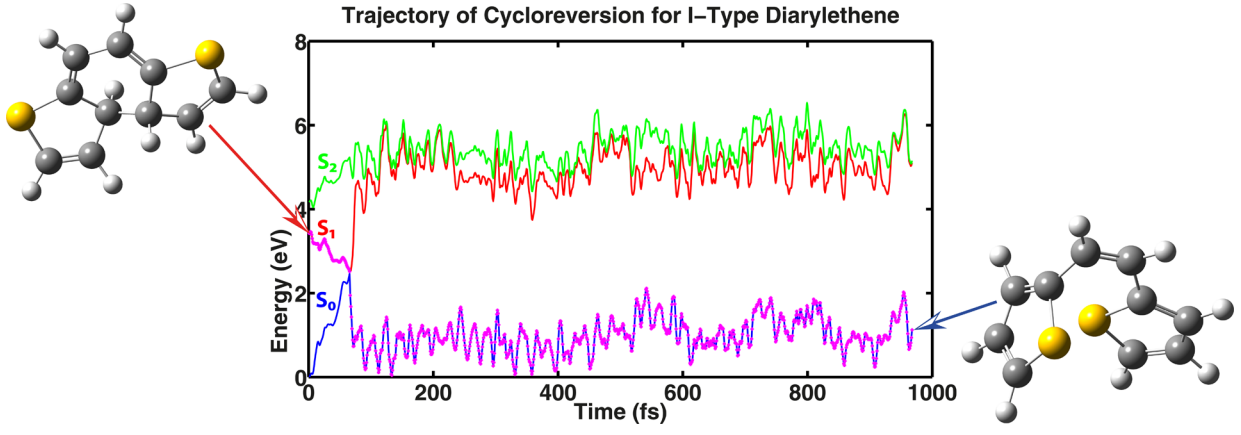

Figure 2. Typical trajectory showing successful cycloreversion for the inverse-type diarylethene (representative of 77% trajectories). Shown is one of the 43 computed trajectories for which the system reacted within a very short time span of only 100 fs. Depicted are the respective energies of S_0, S_1, and S_2 states during the time evolution. After the system passes the conical intersection of S_0 and S_1, the energy separation between S_0 and S_1 significantly increases (compared to the initial separation at $t = 0$), indicative of the cycloreversion reaction. This is confirmed by the initial (closed-ring form) and final (open-ring form) molecular geometries.

dx.doi.org/10.1021/jp506316w | J. Phys. Chem. A 2014, 118, 7816−7823

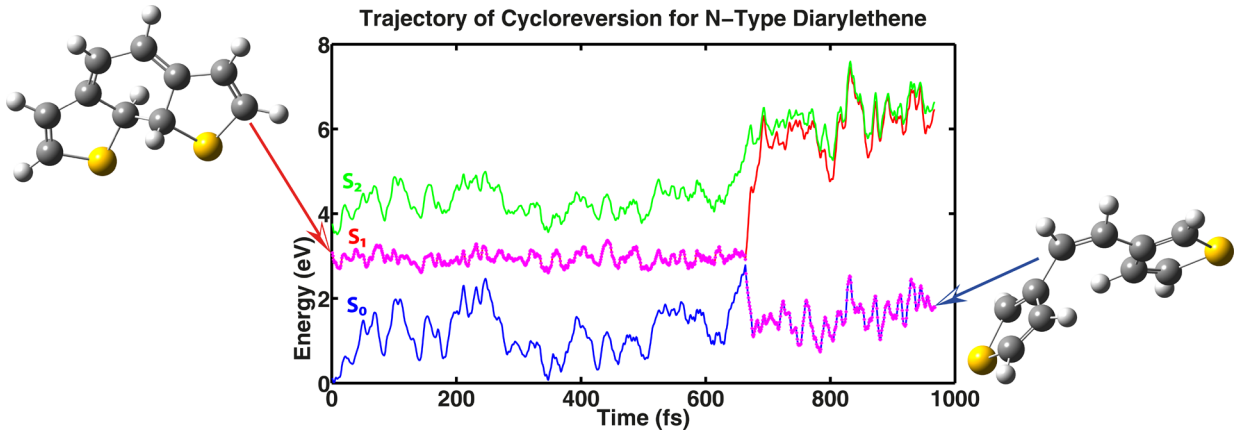

Figure 3. Typical trajectory for successful cycloreversion of the normal-type diarylethene (representative of 55% of trajectories). Here, the typical reaction is significantly slower than for the inverse-type shown in Figure 2.

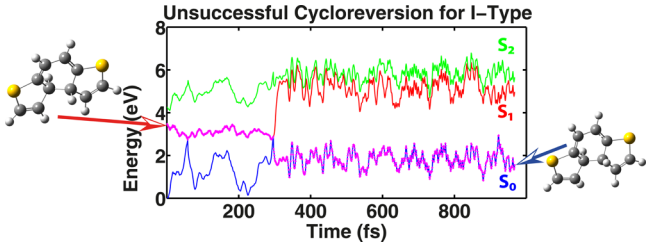

Figure 4. Trajectory for I-type diarylethene that does not reach the ground state within the first 100 fs. The system passes a conical intersection for the first time without relaxing into the ground state. After a while, it reaches the conical intersection for the second time and relaxes back into the closed form, such that no cycloreversion is observed.

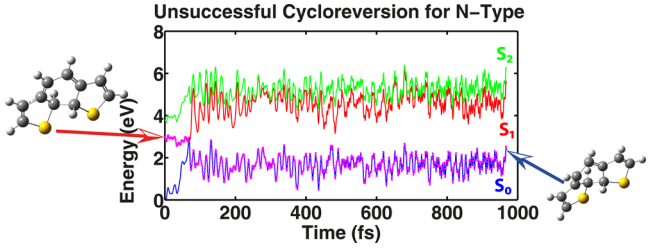

Figure 5. Trajectory for N-type diarylethene that reaches the ground state within 100 fs, not leading to cycloreversion.

semiclassical theoretical approach employed here naturally does not include the true quantized nature of vibrational modes. As a result, the computed reaction time scales are expected to be slightly too fast and the computed excited-state lifetimes underestimated.[51] We note that alternative methods that treat the motion of nuclei more rigorously are Ab Initio Multiple Spawning[67] and Multiconfiguration time-dependent Hartree (MCTDH).[68]

Ultrafast dynamics of the photochemical reactions of diarylethenes were previously investigated in a number of experimental studies (e.g., chapter 12 in ref 6) using, e.g., transient absorption spectroscopy[8,62,69] and femtosecond electron crystallography.[70] Our findings on the reaction dynamics of diarylethenes as discussed above are in accord with previous experimental findings and demonstrate the capabilities of the theoretical approach employed here.

C. Potential Energy Surfaces. To further deepen our understanding of the different dynamics found in N- and I-type diarylethenes, it is instructive to compare the potential energy surfaces for the ground and first excited states. A corresponding relaxed ground-state potential energy surface scan of the energies for varying distance of the two reactive carbon atoms is shown in Figure 6. As expected, we find two almost equally

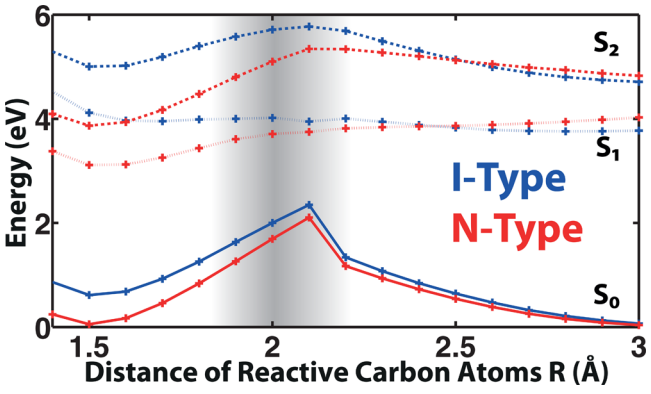

Figure 6. Potential energy surfaces of the normal- (red) and inverse-type (blue) diarylethenes obtained by optimizing the ground-state geometry for varying distances between the reactive carbon atoms. Shown are ground S_0 (solid) and excited S_1 (dotted) and S_2 (dashed) states. Clearly visible is the different topology of the S_1 PES for normal- and inverse-type at $R < 2.1$ Å. To reach the conical intersection between S_0 and S_1 at $R \approx 2.1$ Å in the cycloreversion reaction, for the normal-type diarylethene a potential barrier has to be overcome in the S_1 state. This barrier is absent for the inverse-type diaryethene, leading to a significantly faster and more effcient cycloreversion.

stable ground-state geometries. Vertically exciting the systems from the closed ring form (from the minimum of the ground-state PES at small R) to the first excited state, we find that for the N-type diarylethene a barrier in energy of about 0.6 eV has to be overcome to reach the conical intersection at $R \approx 2.1$ Å. In contrast, there is only a very small energy barrier in the first excited state for the I-type diarylethene such that the ring-opening reaction is (mostly) "downhill" and thus very efficient.

The same qualitative properties of the potential energy surfaces are also found by using RI-CC2 for geometry optimization and calculation of vertical excitation energies, see Figure S3 in the Supporting Information. The good

dx.doi.org/10.1021/jp506316w | J. Phys. Chem. A 2014, 118, 7816–7823

agreement between RI-CC2 and DFT calculation is rather encouraging for using the computationally much cheaper DFT approach.

To obtain a better understanding of the involved PES, we also calculated scans with DFT and RI-CC2 optimizing the first excited state; see Figure 7 and Figure S4 in the Supporting Information. These scans show that even for the optimized S_1 geometries, there is still a barrier for the cycloreversion reaction of N-Type diarylethenes and that the reaction for I-Type molecules proceeds without a barrier. Again, qualitative agreement between DFT and RI-CC2 is found.

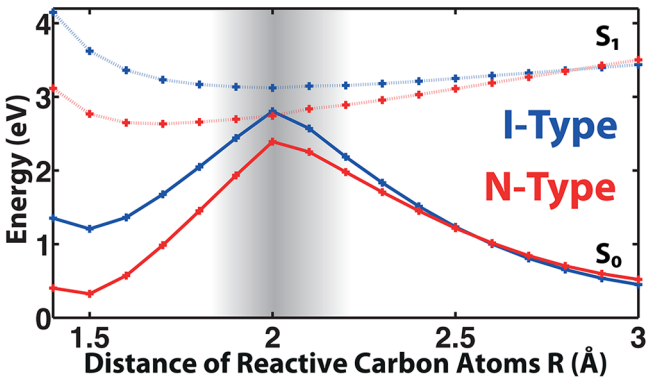

Figure 7. (TD-)DFT calculation of potential energy surfaces obtained by optimizing the first excited state employing TDA. Theses calculations confirm the presence of a potential energy barrier for the normal-type and no barrier for the inverse-type diarylethene when approaching the conical intersection in the S_1 state. The reference energy is the same as for the potential energy surface shown in Figure 6.

We note that in the area shaded in gray in Figures 6 and 7 and in Figures S3 and S4 of the Supporting Information in the vicinity of the conical intersection, our results for the PES based on time-dependent DFT and RI-CC2, respectively, have to be treated with care. Furthermore, the geometry of the conical intersection is a distorted structure[14] such that a PES relaxed on the ground state with vertical excitation energies will not yield this geometry.

The absence of an energy barrier for I-type diarylethenes was already reported before, on the basis of a higher-level quantum chemical approach for a slightly different molecule of this class.[15] We would further like to emphasize that although the difference in reaction efficiencies of I- and N-type can be expected from the PES shown, extraction and prediction of actual numbers for the reaction quantum yields and reaction times is only possible from the full nonadiabatic dynamics calculations as reported here. The actual reaction then takes place on a much more complex, multidimensional PES including all the nuclear degrees of freedom in the system.

IV. CONCLUSION

In this article we report on nonadiabatic ab initio molecular dynamics calculations for the cycloreversion reaction of diarylethenes. We demonstrate that the method employed (trajectory surface hopping based on linear-response time-dependent DFT) is able to reproduce the different dynamics found for N- and I-type diarylethenes. The simulations give detailed insight into the dynamics of the reaction investigated. In particular, reaction quantum yields and reaction times can be extracted that are usually very hard to predict theoretically.

Inspired by these first calculations, there are many future directions that can be addressed. One promising aspect is to study the effect of substitutions at the reactive carbon atoms for N-[71] and I-type[23] diarylethenes for further optimization. Also, detailed studies of the cyclization reaction would be of interest. Apart from its value to the specific field, the present study also constitutes a prime example of the capabilities of high-level available methods in predicting reaction quantum yields and time scales for medium-sized molecular systems.

■ ASSOCIATED CONTENT

Supporting Information

Chemical structures of the diarylethenes studied in experiment used as reference for the excitation energies and for the ultrafast dynamics, a table summarizing the results of Figure 1, videos of the molecular dynamics for the trajectories shown in the text, potential energy surfaces calculated employing RI-CC2 with optimization of the ground and first excited state, respectively, and geometries of the PES obtained by optmizing the first excited state employing TDA. This material is available free of charge via the Internet at http://pubs.acs.org

■ AUTHOR INFORMATION

Corresponding Author

*S. Schumacher. E-mail: stefan.schumacher@uni-paderborn.de.

Notes

The authors declare no competing financial interest.

■ ACKNOWLEDGMENTS

C.W. is grateful for his full PhD-scholarship from the Friedrich-Ebert-Stiftung. We further thank the Turbomole Support team for providing helpful information on the implementation of the TSH-algorithm. We are grateful for fruitful discussions with Prof. Martin J. Paterson, Heriot-Watt University, Edinburgh, UK. Finally, we acknowledge financial support from the DFG (GRK 1464) and a grant for computing time at PC^2 Paderborn Center for Parallel Computing.

■ REFERENCES

(1) Dürr, H., Bouas-Laurent, H., Eds. *Photochromism: Molecules and Systems*; Elsevier: Amsterdam, 2003.

(2) Bianco, A.; Perissinotto, S.; Garbugli, M.; Lanzani, G.; Bertarelli, C. Control of Optical Properties Through Photochromism: a Promising Approach to Photonics. *Laser Photonics Rev.* **2011**, *5*, 711−736.

(3) Nau, D.; Bertram, R. P.; Buse, K.; Zentgraf, T.; Kuhl, J.; Tikhodeev, S. G.; Gippius, N. A.; Giessen, H. Optical Switching in Metallic Photonic Crystal Slabs with Photoaddressable Polymers. *Appl. Phys. B: Laser Opt.* **2006**, *82*, 543−547.

(4) Malic, E.; Weber, C.; Richter, M.; Atalla, V.; Klamroth, T.; Saalfrank, P.; Reich, S.; Knorr, A. Microscopic Model of the Optical Absorption of Carbon Nanotubes Functionalized with Molecular Spiropyran Photoswitches. *Phys. Rev. Lett.* **2011**, *106*, 097401.

(5) Piegdon, K. A.; Lexow, M.; Grundmeier, G.; Kitzerow, H.-S.; Pärschke, K.; Mergel, D.; Reuter, D.; Wieck, A. D.; Meier, C. All-optical Tunability of Microdisk Lasers via Photo-adressable Polyelectrolyte Functionalization. *Opt. Express* **2012**, *20*, 6060−6067.

(6) Irie, M., Yokoyama, Y., Seki, T., Eds. *New Frontiers in Photochromism*; Springer: Tokyo, Japan, 2013.

(7) Irie, M. Diarylethenes for Memories and Switches. *Chem. Rev.* **2000**, *100*, 1685−1716.

(8) Jean-Ruel, H.; Cooney, R. R.; Gao, M.; Lu, C.; Kochman, M. A.; Morrison, C. A.; Miller, R. J. D. Femtosecond Dynamics of the Ring Closing Process of Diarylethene: A Case Study of Electrocyclic

Reactions in Photochromic Single Crystals. *J. Phys. Chem. A* **2011**, *115*, 13158−13168.
(9) Kobatake, S.; Hasegawa, H.; Miyamura, K. High-Convertible Photochromism of a Diarylethene Single Crystal Accompanying the Crystal Shape Deformation. *Cryst. Growth Des.* **2011**, *11*, 1223−1229.
(10) Fukaminato, T.; Kobatake, S.; Kawai, T.; Irie, M. Three-dimensional Erasable Optical Memory using a Photochromic Diarylethene Single Crystal as the Recording Medium. *Proc. Jpn. Acad., Ser. B* **2001**, *77*, 30−35.
(11) Liu, Y.; Lagrost, C.; Costuas, K.; Tchouar, N.; Le Bozec, H.; Rigaut, S. A Multifunctional Organometallic Switch with Carbon-rich Ruthenium and Diarylethene Units. *Chem. Commun.* **2008**, 6117−6119.
(12) Seefeldt, B.; Altenhöner, K.; Tosic, O.; Geisler, T.; Sauer, M.; Mattay, J. Kinetic Studies on Visible-light-switchable Photochromic Fluorophores Based on Diarylethenes. *Photochem. Photobiol. Sci.* **2011**, *10*, 1488−1495.
(13) Aloïse, S.; Sliwa, M.; Buntinx, G.; Delbaere, S.; Perrier, A.; Maurel, F.; Jacquemin, D.; Takeshita, M. Do Inverse Dithienylethenes Behave as Normal Ones? A Joint Spectroscopic and Theoretical Investigation. *Phys. Chem. Chem. Phys.* **2013**, *15*, 6226−6234.
(14) Perrier, A.; Aloïse, S.; Olivucci, M.; Jacquemin, D. Inverse versus Normal Dithienylethenes: Computational Investigation of the Photocyclization Reaction. *J. Phys. Chem. Lett.* **2013**, *4*, 2190−2196.
(15) Nakamura, S.; Uchida, K.; Hatakeyama, M. Potential Energy Surfaces and Quantum Yields for Photochromic Diarylethene Reactions. *Molecules* **2013**, *18*, 5091−5103.
(16) Clayden, J.; Greeves, N.; Warren, S.; Wothers, P. *Organic Chemistry*; Oxford University Press: Oxford, U.K., 2001.
(17) Fleming, I. *Pericyclic Reactions*; Oxford Chemistry Primers; Oxford University Press: Oxford, U.K., 1998.
(18) Woodward, R. B.; Hoffmann, R. The Conservation of Orbital Symmetry. *Angew. Chem., Int. Ed.* **1969**, *8*, 781−853.
(19) Levine, B. G.; Martínez, T. J. Isomerization Through Conical Intersections. *Annu. Rev. Phys. Chem.* **2007**, *58*, 613−634.
(20) Ern, J.; Bens, A. T.; Martin, H.-D.; Mukamel, S.; Tretiak, S.; Tsyganenko, K.; Kuldova, K.; Trommsdorff, H. P.; Kryschi, C. Reaction Dynamics of a Photochromic Fluorescing Dithienylethene. *J. Phys. Chem. A* **2001**, *105*, 1741−1749.
(21) Asano, Y.; Murakami, A.; Kobayashi, T.; Goldberg, A.; Guillaumont, D.; Yabushita, S.; Irie, M.; Nakamura, S. Theoretical Study on the Photochromic Cycloreversion Reactions of Dithienylethenes; on the Role of the Conical Intersections. *J. Am. Chem. Soc.* **2004**, *126*, 12112−12120.
(22) Boggio-Pasqua, M.; Ravaglia, M.; Bearpark, M. J.; Garavelli, M.; Robb, M. A. Can Diarylethene Photochromism Be Explained by a Reaction Path Alone? A CASSCF Study with Model MMVB Dynamics. *J. Phys. Chem. A* **2003**, *107*, 11139−11152.
(23) Tatsumi, Y.; Kita, J.; Uchida, W.; Ogata, K.; Nakamura, S.; Uchida, K. Photochromism of 1,2-Bis(2-thienyl)perfluorocyclopentene Derivatives: Substituent Effect on the Reactive Carbon Atoms. *J. Phys. Chem. A* **2012**, *116*, 10973−10979.
(24) Yuan, K.; Boixel, J.; Le Bozec, H.; Boucekkine, A.; Doucet, H.; Guerchais, V.; Jacquemin, D. Perfluorocyclohexene Bridges in Inverse DiArylEthenes: Synthesis Through Pd-catalysed C-H Bond Activation, Experimental and Theoretical Studies on Their Photoreactivity. *Chem. Commun.* **2013**, *49*, 7896−7898.
(25) Kudernac, T.; Kobayashi, T.; Uyama, A.; Uchida, K.; Nakamura, S.; Feringa, B. L. Tuning the Temperature Dependence for Switching in Dithienylethene Photochromic Switches. *J. Phys. Chem. A* **2013**, *117*, 8222−8229.
(26) Schultz, T.; Quenneville, J.; Levine, B.; Toniolo, A.; Martínez, T. J.; Lochbrunner, S.; Schmitt, M.; Shaffer, J. P.; Zgierski, M. Z.; Stolow, A. Mechanism and Dynamics of Azobenzene Photoisomerization. *J. Am. Chem. Soc.* **2003**, *125*, 8098−8099.
(27) Böckmann, M.; Doltsinis, N. L.; Marx, D. Unraveling a Chemically Enhanced Photoswitch: Bridged Azobenzene. *Angew. Chem., Int. Ed.* **2010**, *49*, 3382−3384.
(28) Böckmann, M.; Doltsinis, N. L.; Marx, D. Nonadiabatic Hybrid Quantum Molecular Mechanic Simulations of Azobenzene Photoswitching in Bulk Liquid Environment. *J. Phys. Chem. A* **2010**, *114*, 745−754.
(29) Toniolo, A.; Levine, B.; Thompson, A.; Quenneville, J.; Ben-Nun, M.; Owens, J.; Olsen, S.; Manohar, L.; Martínez, T. J. Photochemistry from First Principles and Direct Dynamics. *Computational Methods in Photochemistry* **2005**, 167−234.
(30) Wiebeler, C.; Bader, C. A.; Meier, C.; Schumacher, S. Optical spectrum, perceived color, refractive index, and non-adiabatic dynamics of the photochromic diarylethene CMTE. *Phys. Chem. Chem. Phys.* **2014**, *16*, 14531−14538.
(31) Snegir, S. V.; Marchenko, A. A.; Yu, P.; Maurel, F.; Kapitanchuk, O. L.; Mazerat, S.; Lepeltier, M.; Léaustic, A.; Lacaze, E. STM Observation of Open- and Closed-Ring Forms of Functionalized Diarylethene Molecules Self-Assembled on a Au(111) Surface. *J. Phys. Chem. Lett.* **2011**, *2*, 2433−2436.
(32) Tsuboi, Y.; Shimizu, R.; Shoji, T.; Kitamura, N. Near-Infrared Continous-Wave Light Driving a Two-Photon Photochromic Reaction with the Assistance of Localized Surface Plasmon. *J. Am. Chem. Soc.* **2009**, *131*, 12623−12627.
(33) Häser, M.; Ahlrichs, R. Improvements on the Direct SCF Method. *J. Comput. Chem.* **1989**, *10*, 104−111.
(34) Schäfer, A.; Horn, H.; Ahlrichs, R. Fully Optimized Contracted Gaussian Basis Sets for Atoms Li to Kr. *J. Chem. Phys.* **1992**, *97*, 2571−2577.
(35) Perdew, J. P.; Burke, K.; Ernzerhof, M. Generalized Gradient Approximation Made Simple. *Phys. Rev. Lett.* **1996**, *77*, 3865−3868.
(36) Adamo, C.; Barone, V. Toward Reliable Density Functional Methods without Adjustable Parameters: The PBE0Model. *J. Chem. Phys.* **1999**, *110*, 6158−6170.
(37) Furche, F.; Ahlrichs, R. Adiabatic Time-dependent Density Functional Methods for Excited State Properties. *J. Chem. Phys.* **2002**, *117*, 7433−7447.
(38) Hirata, S.; Head-Gordon, M. Time-dependent Density Functional Theory within the Tamm-Dancoff Approximation. *Chem. Phys. Lett.* **1999**, *314*, 291−299.
(39) Dunning, T. H. Gaussian Basis Sets for Use in Correlated Molecular Calculations. I. The Atoms Boron Through Neon and Hydrogen. *J. Chem. Phys.* **1989**, *90*, 1007−1023.
(40) Kendall, R. A.; Dunning, T. H.; Harrison, R. J. Electron Affinities of the First-row Atoms Revisited. Systematic Basis Sets and Wave Functions. *J. Chem. Phys.* **1992**, *96*, 6796−6806.
(41) Christiansen, O.; Koch, H.; Jørgensen, P. The Second-order Approximate Coupled Cluster Singles and Doubles Model CC2. *Chem. Phys. Lett.* **1995**, *243*, 409−418.
(42) Hättig, C.; Weigend, F. CC2 Excitation Energy Calculations on Large Molecules Using the Resolution of the Identity Approximation. *J. Chem. Phys.* **2000**, *113*, 5154−5161.
(43) Hättig, C.; Köhn, A. Transition Moments and Excited-state First-order Properties in the Coupled Cluster model CC2 Using the Resolution-of-the-Identity Approximation. *J. Chem. Phys.* **2002**, *117*, 6939−6951.
(44) Hättig, C. Geometry Optimizations with the Coupled-Cluster Model CC2 Using the Resolution-of-the-Identity Approximation. *J. Chem. Phys.* **2003**, *118*, 7751−7761.
(45) Hättig, C.; Hellweg, A.; Köhn, A. Distributed Memory Parallel Implementation of Energies and Gradients for Second-order Møller-Plesset Perturbation Theory with the Resolution-of-the-Identity Approximation. *Phys. Chem. Chem. Phys.* **2006**, *8*, 1159−1169.
(46) *TURBOMOLE* V6.5 2013, a development of University of Karlsruhe and Forschungszentrum Karlsruhe GmbH, 1989−2007, TURBOMOLE GmbH, since 2007, available from http://www.turbomole.com.
(47) Weigend, F.; Köhn, A.; Hättig, C. Efficient Use of the Correlation Consistent Basis Sets in Resolution of the Identity MP2 Calculations. *J. Chem. Phys.* **2002**, *116*, 3175−3183.

(48) Schirmer, J. Beyond the Random-phase Approximation: A new Approximation Scheme for the Polarization Propagator. *Phys. Rev. A* **1982**, *26*, 2395−2416.
(49) Trofimov, A. B.; Schirmer, J. An Efficient Polarization Propagator Approach to Valence Electron Excitation Spectra. *J. Phys. B: At., Mol. Opt. Phys.* **1995**, *28*, 2299−2324.
(50) Hättig, C. Structure Optimizations for Excited States with Correlated Second-Order Methods: CC2 and ADC(2). *Adv. Quantum Chem.* **2005**, *50*, 37−60.
(51) Tapavicza, E.; Meyer, A. M.; Furche, F. Unravelling the Details of Vitamin D Photosynthesis by Non-adiabatic Molecular Dynamics Simulations. *Phys. Chem. Chem. Phys.* **2011**, *13*, 20986−20998.
(52) Tully, J. C. Molecular Dynamics with Electronic Transitions. *J. Chem. Phys.* **1990**, *93*, 1061−1071.
(53) Jaeger, H. M.; Fischer, S.; Prezhdo, O. V. Decoherence-induced Surface Hopping. *J. Chem. Phys.* **2012**, *137*, 22A545.
(54) Tapavicza, E.; Bellchambers, G. D.; Vincent, J. C.; Furche, F. Ab Initio Non-adiabatic Molecular Dynamics. *Phys. Chem. Chem. Phys.* **2013**, *15*, 18336−18348.
(55) Tapavicza, E.; Tavernelli, I.; Röthlisberger, U. Trajectory Surface Hopping within Linear Response Time-Dependent Density-Functional Theory. *Phys. Rev. Lett.* **2007**, *98*, 023001.
(56) Levine, B. G.; Ko, C.; Quenneville, J.; Martínez, T. J. Conical Intersections and Double Excitations in Time-dependent Density Functional Theory. *Mol. Phys.* **2006**, *104*, 1039−1051.
(57) Tapavicza, E.; Tavernelli, I.; Röthlisberger, U.; Filippi, C.; Casida, M. E. Mixed Time-dependent Density-functional Theory/Classical Trajectory Surface Hopping Study of Oxirane Photochemistry. *J. Chem. Phys.* **2008**, *129*, 124108.
(58) Li, S. L.; Marenich, A. V.; Xu, X.; Truhlar, D. G. Configuration Interaction-Corrected Tamm-Dancoff Approximation: A Time-Dependent Density Functional Method with the Correct Dimensionality of Conical Intersections. *J. Phys. Chem. Lett.* **2014**, *5*, 322−328.
(59) Van Wüllen, C. Shared-Memory Parallelization of the TURBOMOLE Programs AOFORCE, ESCF, and EGRAD: How to Quickly Parallelize Legacy Code. *J. Comput. Chem.* **2011**, *32*, 1195−1201.
(60) Dennington, R.; Keith, T.; Millam, J. *GaussView* Version 5.0.9; Semichem Inc.: Shawnee Mission, KS, 2009.
(61) Kobatake, S.; Yamada, T.; Uchida, K.; Kato, N.; Irie, M. Photochromism of 1,2-Bis(2,5-dimethyl-3-thienyl)-perfluorocyclopentene in a Single Crystalline Phase. *J. Am. Chem. Soc.* **1999**, *121*, 2380−2386.
(62) Ishibashi, Y.; Mukaida, M.; Falkenström, M.; Miyasaka, H.; Kobatake, S.; Irie, M. One- and multi-photon cycloreversion reaction dynamics of diarylethene derivative with asymmetrical structure, as revealed by ultrafast laser spectroscopy. *Phys. Chem. Chem. Phys.* **2009**, *11*, 2640−2648.
(63) Atchity, G. J.; Xantheas, S. S.; Ruedenberg, K. Potential Energy Surfaces Near Intersections. *J. Chem. Phys.* **1991**, *95*, 1862−1876.
(64) Yarkony, D. R. Nuclear Dynamics Near Conical Intersections in the Adiabatic Representation: I. The Effects of Local Topography on Interstate Transitions. *J. Chem. Phys.* **2001**, *114*, 2601−2613.
(65) Ben-Nun, M.; Molnar, F.; Schulten, K.; Martínez, T. J. The Role of Intersection Topography in Bond Selectivity of cis-trans Photoisomerization. *Proc. Natl. Acad. Sc. U. S. A.* **2002**, *99*, 1769−1773.
(66) Lee, A. M. D.; Coe, J. D.; Ho, M.-L.; Lee, S.-J.; Ullrich, S.; Cheng, B.-M.; Zgierski, M. Z.; Chen, I.-C.; Martínez, T. J.; Stolow, A. Substituent Effects on Dynamics at Conical Intersections: α,β-Enones. *J. Phys. Chem. A* **2007**, *111*, 11948−11960.
(67) Ben-Nun, M.; Quenneville, J.; Martnez, T. J. Ab Initio Multiple Spawning: Photochemistry from First Principles Quantum Molecular Dynamics. *J. Phys. Chem. A* **2000**, *104*, 5161−5175.
(68) Beck, M. H.; Jäckle, A.; Worth, G. A.; Meyer, H.-D. The Multiconfiguration Time-dependent Hartree (MCTDH) Method: a Highly Efficient Algorithm for Propagating Wavepackets. *Phys. Rep.* **2000**, *324*, 1−105.
(69) Ishibashi, Y.; Umesato, T.; Kobatake, S.; Irie, M.; Miyasaka, H. Femtosecond Laser Photolysis Studies on Temperature Dependence of Cyclization and Cycloreversion Reactions of a Photochromic Diarylethene Derivative. *J. Phys. Chem. C* **2012**, *116*, 4862−4869.
(70) Jean-Ruel, H.; Gao, M.; Kochman, M. A.; Lu, C.; Liu, L. C.; Cooney, R. R.; Morrison, C. A.; Miller, R. J. D. Ring-Closing Reaction in Diarylethene Captured by Femtosecond Electron Crystallography. *J. Phys. Chem. B* **2013**, *117*, 15894−15902.
(71) Morimitsu, K.; Kobatake, S.; Irie, M. Control of Cycloreversion Quantum Yields of Diarylethenes by Introduction of Substituents at the Reactive Carbons. *Mol. Cryst. Liq. Cryst.* **2005**, *431*, 151−154.